Behavior of geosynthetic encased stone columns (GESC) under cyclic loading: Experimental study

Qaisar Abbas & Chungsik Yoo
Department of Civil, Architectural and Environmental Engineering, Sungkyunkwan University, Korea

ABSTRACT: Geosynthetic encasement around the stone columns in weak and lose ground can provide the additional confinement to the stone columns thus increasing their load carrying capacity and reducing lateral and vertical deformation. Studies on the stone columns under static loading are well known but the bearing mechanism of GESC under cyclic loading is not yet fully understood and cannot be forecasted. This research presents the results of an investigation on the load-bearing capacity, and reduction of vertical and lateral deformation of GESC under cyclic loading based on the laboratory reduced scale model tests. Based on the results of present investigation, it is seen that the stone column ultimate load reduced up to 34% under cyclic loading as compared to static loading but it can be confined by using proper stiffness geosynthetic encasement up to 25% as compared to without encasement (OSC).

Keywords: Geosynthetics, Cyclic loading, Reduced-scale model test, geosynthetic encased stone column

1 INTRODUCTION

Recently for the improvement of lose and soft ground, the stone column technique has been widely used as method of reinforcing the ground for different facilities like highway, bridges, railway embankments, bridge abutments and foundation constructions. Stone columns are usually provided to increase the bearing capacity of surrounding ground, reduce the settlement and to improve the lose ground. The most common failure mechanism in the granular piles as well as stone column is bulging failure regardless of whether it is floating or end bearing (Madhav and Vanitha 2006). These days, the concept of granular piles or stone columns encasing with geosynthetic over the full or partial height of stone column to increase the bearing capacity of stone columns has been studied by many researchers (Kempfert et al. 1997; Raithel and Kempfert 2000; Kempfert and Raithel 2002; Raithel et al. 2002; Murugesan and Rajagopal 2007; Yoo. 2010; Gniel and Bouazza 2010; Yoo and Lee 2012; Ali et al. 2012, 2014; Chen et al. 2015; Gu et al 2016; Ou et al. 2017).

Even though there are many studies available on ordinary stone columns (OSC) as well as geosynthetic encased stone columns (GESCs) and provided valuable information for the construction of stone columns as well as to check the behavior under different conditions as reported by (Hanna et al. 2013; Mohapatra and Rajagopal 2017). But based on previous studies literature review, it is found that the behavior of GESCs under cyclic loading is not fully understood and almost there is no study available on GESC under repeated loading. By considering the cyclic loading impact on stone column, the current study has been carried out by using the GESCs to improve the ground under cyclic loading.

In the present study, A series of model test box experiments were performed in laboratory to understand the behavior of GESCs under cyclic loading. To investigate the performance of stone column under cyclic loading as well as the effect geosynthetic encasement to improve the bearing capacity of stone column, the experiments were performed under effect of cyclic and static loading as well as under the effect of different geogrid stiffness. The results were presented in form of time variation of load, settlement, stress concentration ratio (n), pressure sharing ratio and hoop strain to better understand the stone column behavior under cyclic loading.

2 LABORATORY MODEL TEST

2.1 *Materials properties*

2.1.1 *Model ground and stone column material*

In present study, the model ground was prepared with fine dry sand classified as SP based on unified soil classification system (USCS ASTM 2487-11 2011) with effective particles size of (D_{10}) 0.44mm, the co-efficient of uniformity of (C_u) 1.41 and coefficient of curvature of (C_c) 0.92. For the preparation of stone column, the angular crushed aggregates used in present study with an effective particle size of 10-40mm and classified as GP based on unified soil classification system (USCS). The geotechnical properties of model ground sand and stone column crushed aggregates shown in Table 1.

Table 1. Materials Properties

Properties	Sand	Aggregates
Specific gravity	2.63	2.6
Particle size distribution		
Percentage aggregates[4.75-80mm]	-	100
Percentage sand [0.425-4.75mm]	0	0
Percentage sand [0.075-0.425mm]	100	0
D_{10} [mm]	0.44	13
D_{30} [mm]	0.51	31
D_{60} [mm]	0.62	39
Coefficient of uniformity C_u	1.41	3
Coefficient of curvature C_c	0.92	1.89
Soil classification USCS	SP	GP
Compaction characteristics		
Max. dry unit weight,	16.8 [D_r = 50%]	21
Frictional characteristics		
Cohesion c (kPa)	0	5
Internal friction angle, ϕ (degree)	35 [D_r = 50%]	41

2.1.2 *Geosynthetic reinforcement*

A polyethylene biaxial geogrid was used in the model test to create the geosynthetic encasement of 50 mm diameter. Two types of geogrids were used to create the encasement, full-scale geogrid with aperture size 25 x 25 mm and reduced scale geogrid with aperture size 50 x 50 mm by cutting the full-scale geogrid into half as shown in Figure 1(a) and (b) to achieve the possible effect of similitude law application on a reduced scale. The tensile strength of geogrid was measured by standard wide width tensile test method (ASTM 4595 2011) and from results of wide width tensile test results, it is observed that tensile strength of geogrid on a RGG, reduced up to 50% as compared to FGG. From wide width tensile test with nylon ties, it is seen that the tensile strength of geogrid remains same with and without ties within the limit of up to 1% as shown the results in Figure 1(c)

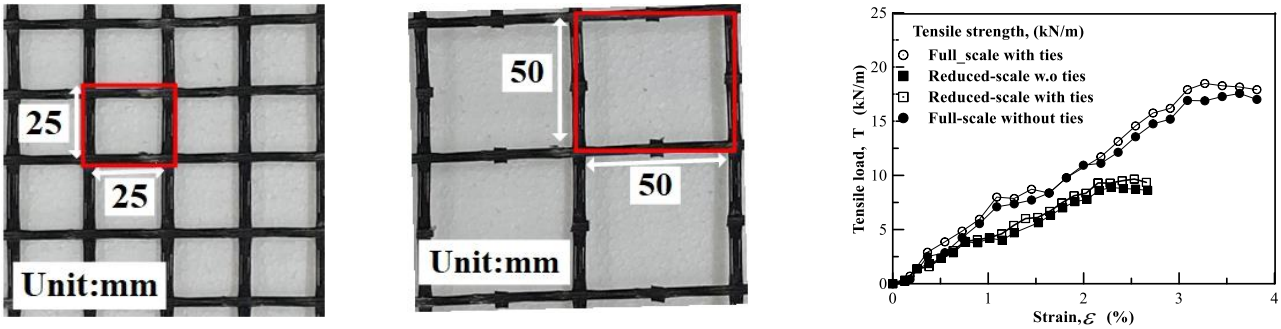

(a) Full geogrid (FGG) (b) Reduced grid geogrid (RGG) (C) Tensile test results

Figure 1. Aperture size and tensile strength results of used geogrid in model test

2.2 *Experiment setup and test procedure*

2.2.1 *Geosynthetic encasement preparation*

The geosynthetic encasement was formed by rolling the flat geogrid into the cylindrical form to make the 50 mm diameter geosynthetic encasement. The geogrid sleeve in circumferential direction had a 30% overlapping and nylon ties were used to fix the geogrid sleeve in the position to prevent the encasement unraveling during the construction of column and under loading. The vinyl wrap around the geogrid encasement was used to prevent the stone movement out of the geogrid especially in case of reduced-scale geogrid due to large opening as shown in the flat geogrid configurations and geogrid encasement in Figure 2(a) and (b). Further to check the effect of vinyl wrapping around the encasement, the stone column test was performed with full geogrid with and without vinyl wrap under cyclic loading conditions as given in Figure 4 and the results are shown in Figure 2(c). To check the effect of vinyl wrapping around the encasement, the settlement results with and without wrapping are almost equal within permissible limit of 1-2% (Figure 2(c)). From the results of the tensile strength of geogrid for binding ties and stone column with vinyl wrapping, it is suggested that nylon ties as binding and vinyl wrap as the encasement wrapping, to prevent the stone movements out of the geogrid, can be used in the model test.

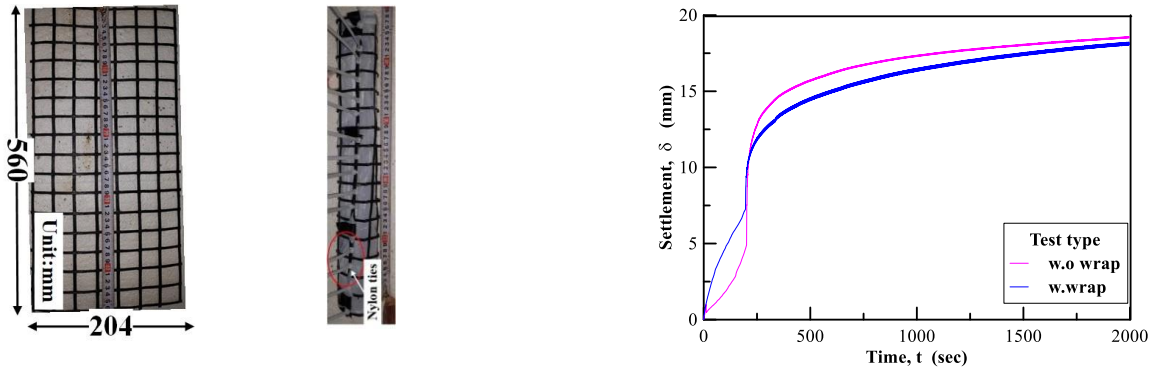

(a) Flat geogrid (b) Encasement (C) Settlement of column with and without vinyl wrap

Figure 2. Geosynthetic encasement and test results for vinyl wrap effect

2.2.2 *Model ground and stone column preparation*

The sand model ground for geosynthetic encased stone column was prepared in a circular oedometer tank made of 50 mm thick steel plate with a diameter of 280 mm and height of 580 mm as shown in Figure 3(a) to achieve the possible effect of similitude law application. Before the preparation of model ground a 600 mm steel casing with an outer diameter of 52 mm was placed in the center of test box along with geosynthetic encasement with 50 mm diameter inside the casing. After the installation of casing, the model ground was prepared in layers to achieve the relative density of 50% against the dry unit weight of 17kN/m^3. After the preparation of sand model ground outside the steel casing, the stones aggregates with size of 2-10 mm were poured into the casing with proper compaction to achieve the 90% degree of compaction against 20kN/m^3 unit weight of crushed aggregates. The 560 mm long stone column was prepared in 7 layers with 80 mm height of each layer and the casing was moved up with same height after the preparation of each layer up to the final layer. During the preparation of pressure sensor were installed in to the stone column as well as model ground to measure the stress concentration ratio as well as pressure sharing ratio in column. After the preparation of stone column and model ground, the thin 10 mm sand layer was placed on the top to make the flat surface for uniform loading and applied the loading on stone column with 100 mm diameter loading plate by considering the 25% area replacement ratio as the schematic view of detail test setup shown in Figure 3(b).

2.2.3 *Monitoring program*

To monitor the performance of GESC under cyclic loading, the hoop strain (ε_g) was measured by strain gauges attached along the circumferential direction of geogrid at 1.0D (50mm below the loading plate, S1), at the 5.6D (mid-depth, S2) and 10D (near to the bottom, S3). The strain gauges along the encasement were attached by special epoxy glue and transparent tape to make the strain gauge fully covered as shown in Figure 4(a) and for the measurement of pressure sharing ratio in column and stress concentration ratio between the column and model ground soil three pressure sensor were installed in stone column and three in model ground as the pressure sensor and detail instrumentation program shown in Figure 3(b).

The NI cDAQ-9174 data logger was used to measure the pressure and strain in geogrid as shown in Figure 4(b).

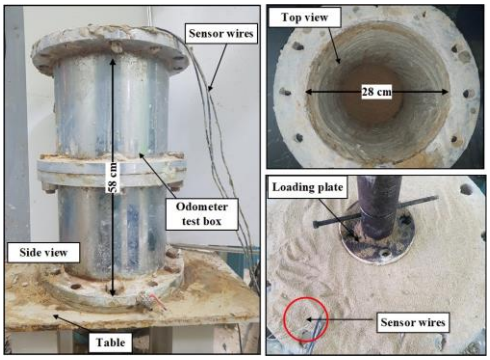

(a) Test box configurations

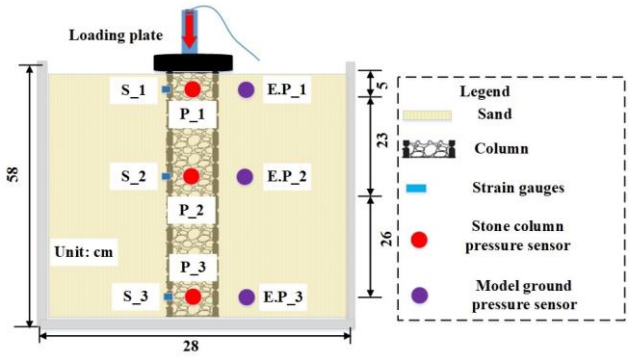

(b) Schematic view of test setup

Figure 3. Test box configurations and schematic view of test setup

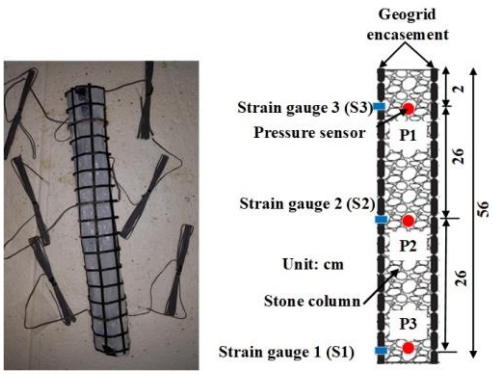

(a) Strain gauge and pressure sensor arrangement

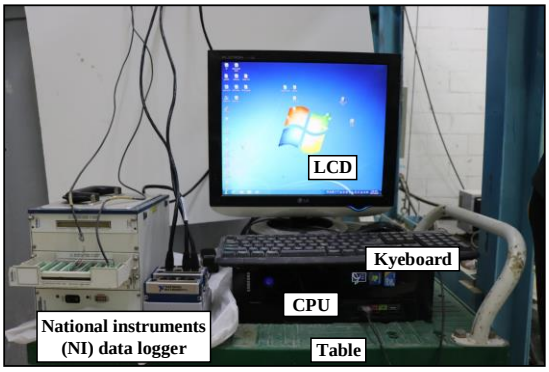

(b) Data logger

Figure 4. Strain gauges arrangement and data logger

2.3 *Loading conditions*

The load on the stone column was applied by using 100 mm loading plate with 25% area replacement ratio, A_r (Ratio of area of column to influence area under loading) suggested by (Ali et al. 2012), to apply the load eccentrically. The load was applied with hydraulic jack loading system capable of applying monotonic and cyclic loading having 20-ton capacity load cell and 200 mm gauge length LVDT.

In present study, the load was applied based on the ultimate load of stone column. To check the ultimate load of stone column, the laboratory experiment was performed with static loading and without geosynthetic encasement as the results shown in Fig. 5(a). In static loading case the load was applied at rate of 1.0mm/min and from the results of static load experiment, the ultimate load (P_u) was determined as 5kN which is by chance equal to calculated load. The cyclic load was applied as $0.7P_u$ as maximum load (P_{max}) and $0.3P_u$ as a min load (P_{min}). To achieve the $P_{max} = 0.7P_u = 3.5$kN and $P_{min} = 0.3P_u = 1.5$kN, the 1kN half sin wave amplitude was selected with initial loading value of 2.5kN. Typically, cyclic loading conditions, loading frequency of f =0.5Hz with 10800 loading cycles to properly check the behavior of GESC under cyclic loading were selected. To achieve the above cyclic loading conditions, the load was applied in three steps, in loading step_1, the load was applied linearly to reach up to, $P_{initial} = 2.5$kN in loading step_2, the load control automatically changed to sine wave control to achieve the required cyclic loading conditions and after cyclic loading in loading step_3, the linear load was continued at a rate of 1.0 mm/min to see the post cyclic ultimate load of stone column as shown the loading steps in Fig. 5(b).

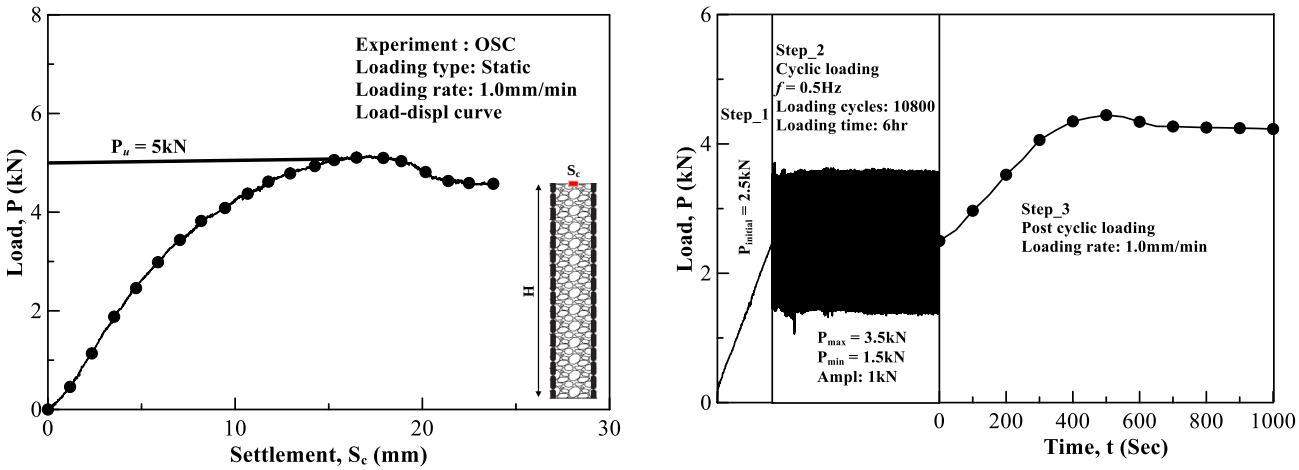

(a) Determination of ultimate load (P_u) (b) Cyclic loading conditions

Figure 5. Loading conditions used in laboratory model test

2.4 *Parametric study*

To investigate the effect of geosynthetic encased stone column under cyclic loading, the laboratory experiments were performed by considering the effect of cyclic loading (Series A) and effect of geogrid stiffness (Series B). The detail experimental plan shown in Table 2.

Table 2. Parametric study.

Series	Column type	Loading	GG type	Dr (%)	*f* (Hz)	N	Amplitude
A	OSC	S_L	-	50	0.5	-	-
	OSC	C_L	-			10800	±1
	GESC	S_L	RGG			-	-
	GESC	C_L	RGG			10800	±1
B	OSC	C_L	-	50	0.5	10800	±1
	GESC		RGG				
	GESC		FGG				

Note: GESC: Geosynthetics encased stone column; OSC: Ordinary stone column; FGG: Full grid geogrid; RGG: Reduced grid geogrid; SL: Static loading; CL: Cyclic loading; GG: Geogrid: Dr: Relative density; *f*: Frequency; N: Loading cycles

3 RESULTS AND DISCUSSION

3.1 *Effect of cyclic loading*

To check the effect of cyclic loading the laboratory model test box experiment was performed for GESC and OSC under both static and cyclic loading conditions as given above in Figure 5. The results were drawn for time variation of load to check the variation of post cyclic ultimate load as the results shown in Figure 6. From results it is seen that the stone column ultimate load significantly reduced after the cyclic loading as compared to static loading. Further to more clearly demonstrate the post cyclic ultimate load results, the results were drawn in term of maximum ultimate load for static and post cyclic ultimate load and also for percentage ultimate load reduction with respect to static loading as the results shown in Figure 7.

From presented results for OSC and GESC under static and cyclic loading, it is seen that load bearing capacity of stone column significantly increase with geosynthetic encasement as compared to ordinary stone column (OSC) for both cyclic and static loading. From percentage reduction results it is seen that, post cyclic ultimate load reduction in case of GESC is 25% but the ultimate load reduction is up to 34% with respect to static loading.

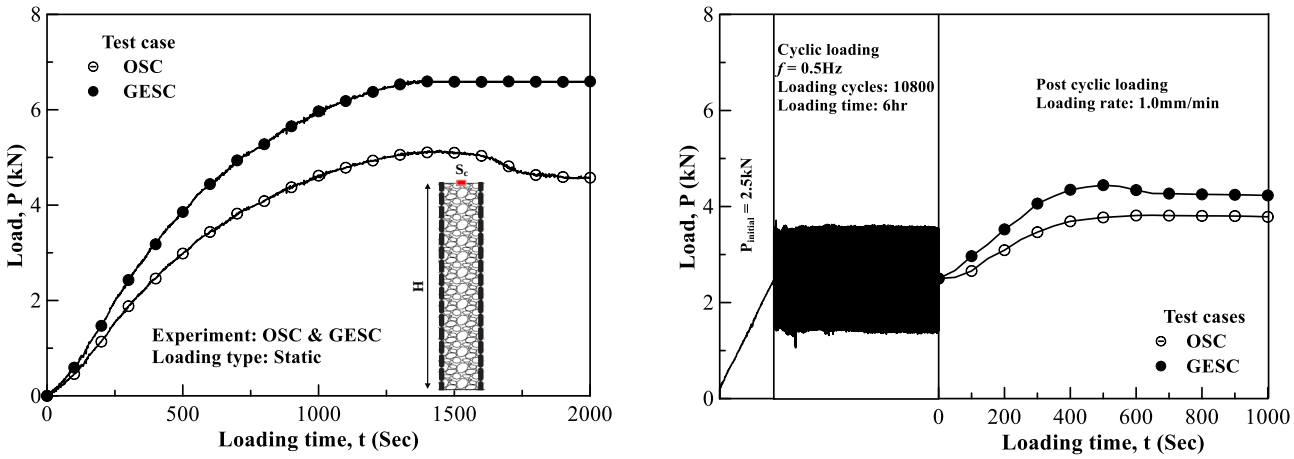

(a) Load variation under static loading (b) Post cyclic ultimate load

Figure 6. Time variation of load under static and cyclic loading

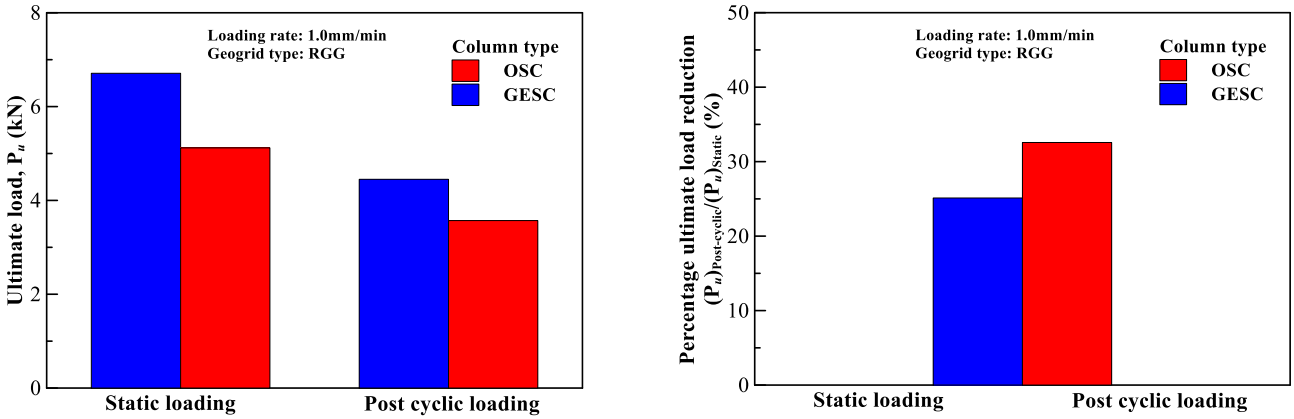

(a) Max. ultimate load (b) Reduction with respect to static load

Figure 7. Ultimate load and percentage reduction of post cyclic ultimate load with respect to static

3.2 *Effect of geogrid stiffness*

To investigate the effect of geogrid encasement stiffness on the performance of stone column under cyclic loading the experiment was performed for OSC, GESC experiment with full and reduced grid geogrid and the results were presented in form of post cyclic ultimate load, stone column settlement, stress concentration ratio and pressure sharing ratio.

The time variation of post cyclic ultimate and percentage increase of post cyclic ultimate load with different stiffness encasement with respect to OSC shown in Figure 8 and from results it is seen that the settlement significantly increases with higher stiffness encasement. From percentage increase of ultimate load, it is seen that the 16% load increase in case of RGG and 29% in case of FGG with respect to OSC.

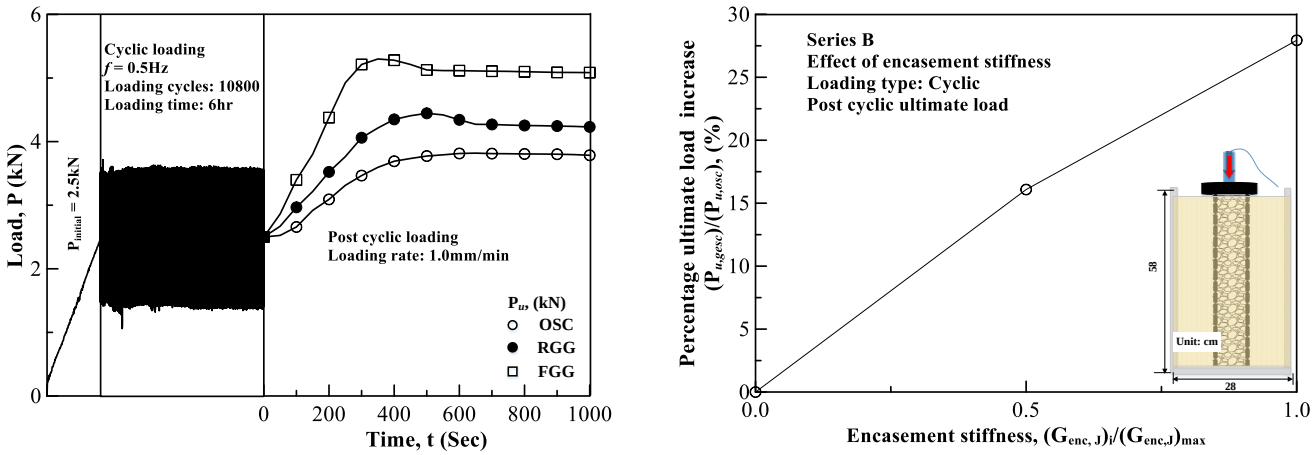

(a) Post cyclic ultimate load (b) Percentage increase of load

Figure 8. Post cyclic and percentage increase of post cyclic ultimate load under encasement stiffness

The time variation of stone column settlement and percentage reduction of stone column settlement shown in Figure 9. From results it is seen that stone column settlement significantly reduced by increasing the stiffness of geosynthetics encasement as the stone column settlement significantly large in case of OSC and significant stone column settlement reduction occur with encasement even with reduced grid geogrid. From the percentage settlement reduction of settlement with respect to OSC, it is seen that 26% settlement reduction in case of RGG and 37% in case of FGG (Figure 9(b)).

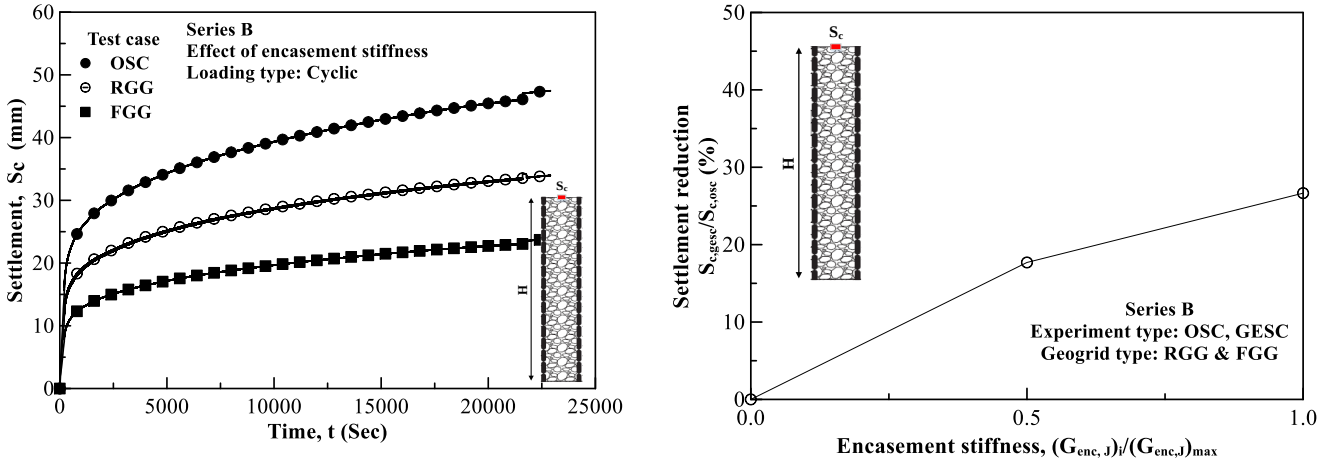

(a) Stone column settlement (b) Increase of stone column settlement

Figure 9. Time variation and percentage increase of stone column settlement

Figure 10 show the results for percentage increase of stress concentration ratio ($n = \sigma_{v,c}/\sigma_{v,s}$) between the column and soil and the pressure sharing ratio along the column from top to bottom compare at P1 under pre-cyclic, cyclic and post cyclic load. From results of stress concentration ratio, it is seen that the SCR significantly increases with the increase of encasement stiffness with respect to OSC almost up to 41% in case of RGG and 63% incase of FGG (Figure 10(a)). The percentage increase of pressure sharing ratio (PSR) results shown in Figure 10(b) and from results it is seen that the pressure sharing ratio significantly increases with the increase of encasement stiffness almost up to 25% as compared to OSC. Which shows the significance of geosynthetic encasement as the encasement increase the confining stress of stone column and maximum applied pressure goes to stone column and surrounding soil remain safe in term of bearing capacity.

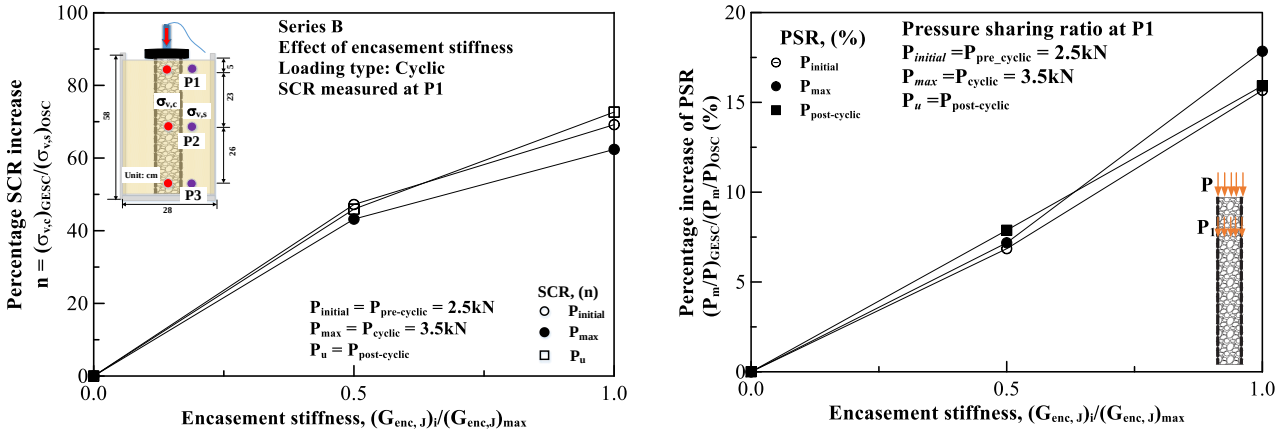

(a) Stress concentration ratio (b) Pressure sharing ratio

Figure 10. Percentage increase of SCR and PSR with encasement with respect to OSC

4 CONCLUSIONS

A series of reduced scale model test box experiments were performed to check the relative effect of cyclic loading on stone column by considering the effect of cyclic loading and geogrid stiffness. To check the effect of cyclic loading on stone column, the OSC and GESC test was performed under static and cyclic loading and from results, it is investigated that, significant ultimate load reduction under cyclic loading as compared to static loading. From the effect of geogrid encasement stiffness, the post cyclic ultimate load significantly increases with the increase of encasement stiffness up to 29% and similarly the stone column

settlement reduced up to 37% with respect to OSC. The stress concentration ratio and pressure sharing ratio also significantly increase by increasing the stiffness of encasement from OSC to full geogrid encasement which shows the importance of encasement stiffness as by increasing the encasement stiffness the load carrying capacity of stone column increase.

ACKNOLDGEMENT

This research was supported by the Korea Agency for Infrastructure Technology Advancement under the Ministry of Land, Infrastructure and Transport of the Korean government. (Project Number: 17SCIP-B108153-03)
This research is supported by (NRF-2017R1E1A1A01077246) from the Basic Research Program of the Korea Science & Engineering Foundation. The financial supports are gratefully acknowledged.

REFERENCES

Ali, K., Shahu, J. T. and Sharma, K. G. (2012). Model tests on geosynthetic-reinforced stone columns: a comparative study. Geosynthetics International, 19, No. 4, 292–305.
Ali, K., Shahu, J. T. & Sharma, K. G. (2014). Model tests on single and groups of granular columns with different geosynthetic reinforcement arrangement. Geosynthetics International, 21, No. 2, 103–118.
Chen, J. F., Li, L. Y., Xue, J. F. & Feng, S. Z. (2015). Failure mechanism of geosynthetic-encased stone columns in soft soils under embankment. Geotextiles and Geomembranes, 43, No. 5, 424–431.
Gneil, J. & Bouazza, A. (2010). Construction of geogrid encased stone columns: A new proposal based on laboratory testing. Geotextiles & Geomembranes, 28, No. 1, 108–118.
Gu, M., Zhao, M., Zhang, L. and Han, J. (2016). Effects of geogrid encasement on lateral and vertical deformations of stone columns in model tests. Geosynthetics International, 23, No. 2, 100–112.
Hanna, A. M., Etezad, M. & Ayadat, T. (2013). Mode of failure of a group of stone columns in soft soil. International Journal of Geomechanics, 13, No. 1, 87–96.
Kempfert, H. G., Jaup, A. & Raithel, M. (1997). Interactive behavior of a flexible reinforced sand column foundation in soft soils. International Conference on Soil Mechanics and Foundation Engineering, ISSMGE, Hamburg, Germany, Vol. 14, pp. 1757–1760.
Kempfert, H. G. & Raithel, M. (2002). Experiences on dike foundations and landfills on very soft soils. Technical Committee TC 36 Soft Soils Foundation Engineering. International Symposium on Soft Soils Foundation Engineering, Mexico City, Mexico, pp. 176–181.
Murugesan, S. & Rajagopal, K. (2007). Model tests on geosynthetic encased stone columns. Geosynthetics International, 14, No. 6, 346–354.
Mohapatra, S. R. and Rajagopal, K. (2017). Undrained stability analysis of embankments supported on geosynthetic encased granular columns. Geosynthetics International, 24, No. 5, 465–479.
Madhav, M.R. & Vanitha, L. (2006). Analysis and design of granular pile reinforced ground. Proceedings, ATC-7 Workshop on Stone Column in Soft Deposits, Busan, Korea, pp. 1–17.
Ou Yang, F., Zhang, J. J., Liao, W. M., Han, J. W., Tang, Y. L. and Bi, J. B. (2017). Characteristics of the stress and deformation of geosynthetic-encased stone column composite ground based on large-scale model tests. Geosynthetics International, 24, No. 3, 242–254.
Raithel, M. & Kempfert, H. G. (2000). Calculation models for dam foundations with geotextile-coated sand co umns. Proceedings of GeoEngineering 2000, Melbourne, Australia, pp. 347.
Raithel, M., Kempert, H. G. & Kirchiner, A. (2002). Geotextile-encased columns (GEC) for foundation of a dike on very soft soils. Geosynthetics – State of the Art Recent Developments, Delmas, P., Gourc, J. P. & Girard, H., Editors, Balkema, Rotterdam, the Netherlands, pp. 1025–1028.
Yoo, C. & Lee, D. (2012). Performance of geogrid-encased stone columns in soft ground: full-scale load tests. Geosynthetic International, 19, No. 6, 480-490.
Yoo, C. (2010). Performance of geosynthetic-encased stone columns in embankment construction: numerical investigation. Journal of Geotechnical and Geoenvironmental Engineering, 136, No. 8, 1148–1160.